Infrared Spectra and Structures of the Valyl-Alanine and Alanyl-Valine Zwitterions Isolated in a KBr Matrix

Rebecca Jacob[†] and Gad Fischer*

Department of Chemistry, The Faculties, The Australian National University, Canberra ACT 0200, Australia

Received: December 19, 2002; In Final Form: May 6, 2003

The infrared absorption spectra of the dipeptide zwitterions L-valyl-L-alanine and L-alanyl-L-valine have been measured using a novel infrared sampling technique. The two dipeptides are isomers, and similar spectra are expected and were measured. With the better resolved spectra obtained with the dissolution, spray, and deposition technique, small but significant differences were identified, not evident in the normal KBr pellet spectra. Ab initio molecular orbital calculations of the self-consistent reaction field type using the Onsager dipole−sphere model were undertaken for structure determinations and spectral predictions at Hartree−Fock and density functional theory levels. A number of conformers were identified; the structure of the calculated most stable one of L-valyl-L-alanine was found to be in excellent agreement with the X-ray crystallographically determined bond length and angles. The spectral resolution obtained, together with theoretical predictions of the absorption spectra, and comparisons with the spectra of related dipeptides and amino acids have enabled vibrational assignment of bands and identification of molecular conformers.

Introduction

Knowledge of the vibrational spectra and structures of the amino acids and peptides is very necessary in areas such as the construction of three-dimensional models of protein structures and in studies of the photosynthetic reaction center. In traditional methods, vibrational spectra have been measured in pressed pellets, usually KBr, in liquid hosts such as Nujol, and in solution. In these methods, the spectra refer to the zwitterions significantly perturbed by neighboring zwitterions or by solvent molecules. As a consequence, the spectra are typically characterized by broad and partly structured absorption bands extending from about 3300 to 2300 cm^{-1}. At lower frequencies (1700 to 400 cm^{-1}), better resolution is achieved and some individual bands may be identified.

Evidence from structure calculations and from experiment suggests that the zwitterions are not stable in the absence of a dielectric field and that they revert to the neutral form.[1−12] The dielectric field is provided by neighboring molecules in the solid and by polar solvent molecules in solution. Few spectral studies have been reported for the neutral molecules, largely because the measurements must be conducted for isolated molecules. This condition is achieved in the vapor phase and in low temperature inert gas matrixes, but studies are limited because of the relatively low thermal stabilities of the amino acids and peptides.

We have recently developed a spray sampling technique, which has been spectacularly successful in producing resolved infrared (IR) absorption spectra throughout the mid-IR range.[13] We have argued that the spectra so obtained refer to isolated zwitterions stabilized by the dielectric field of the alkali halide matrix. The technique, which has similarities to the low temperature isolation of molecules in inert gas matrixes, has been applied to a number of amino acids[13−18] and dipeptides.[19,20] The resolution obtained, together with theoretical predictions of the absorption spectra, has enabled vibrational assignment of bands and identification of molecular conformers.

In this work, we apply the method to the study of the dipeptides L-valyl-L-alanine (val-ala) and L-alanyl-L-valine (ala-val). The two molecules are isomers and have identical atomic chains linking the terminal NH_3^+ and CO_2^- groups. Although the isomers possess the same side chains, they differ in their disposition, in that the groups methyl of alanine and isopropyl of valine interchange. Thus, it could be anticipated that the vibrational spectra should be very similar. IR absorption spectroscopy can confirm this, and the much better spectral resolution achieved using our spray sampling technique allows spectral differences to be identified that would not be observed using the standard KBr pellet method.

Finally, comparisons are undertaken with the similarly obtained spectra of the related molecules, glycyl-L-alanine (gly-ala),[19] L-valyl-glycine (val-gly),[20] and L-alanine.[16] They assist in the vibrational assignments, help in the analyses of the standard (KBr) pellet spectra, and identify trends in frequencies and intensities of specific vibrations among the amino acids and dipeptides.

Experimental Section

In the measurement of the IR absorption spectra, samples were obtained by the dissolution, spray, and deposition method (DSD), which required preparation of solutions that are very dilute in the dipeptide but near-saturated in alkali halide. These solutions were then deposited by very fine spray on to IR transparent disks. The disks were held at elevated temperatures, 60 °C in this work, to facilitate removal of water. This is a lower temperature than that used in previous studies of the amino acids[13−18] because of our concerns regarding the thermal stability

* To whom correspondence should be addressed. Tel: + 61 2 6125 2935. Fax: + 61 2 6125 0760. E-mail: Gad.Fischer@anu.edu.au.

[†] On leave from the Department of Chemistry, Madras Christian College, Tambaram, Chennai, 600 059, India.

10.1021/jp0226275 CCC: $25.00
Published on Web 07/22/2003

of the dipeptides. To ensure that the deposits on the disks contained no water, an additional step was introduced in the sample preparation. Following each of the successive spray depositions, the disks were subjected to vacuum-drying. Additional details on the preparation of DSD samples have been previously reported.[13] Crystalline val-ala and ala-val were obtained from ICN and used without further purification. In this work, aqueous solutions were used, and the matrix and window were KBr (Fourier transform (FT)-IR grade, Aldrich). Molar ratios of KBr to dipeptide were in the range of 1000−1500. No decomposition products were detected in the IR spectra. By means of this technique, it is suggested that largely monomers of the dipeptide zwitterions isolated in a film of KBr were obtained.

It should be noted that dissolution of the two dipeptides in aqueous solutions at 60 °C did not lead to any chemical changes. This was checked by measurement of the KBr pellet spectra of the sample remaining after the DSD solutions had been evaporated to dryness at the same temperature. The spectra were identical to those using the standard KBr pellet method but different from the DSD spectra. Not only did this indicate that no decomposition had taken place but it showed that the DSD spray technique produced sample molecules in different molecular environments to simple evaporation.

IR spectra were measured with an FT-IR spectrometer (Bruker IFS66) at a resolution of 4 cm^{-1}, over the full mid-IR range (4000−400 cm^{-1}). Because of low absorbances resulting from the use of very dilute solutions and thin sprays, repeated scans (500−1000) were run to maximize signal-to-noise. The standard KBr pellet spectra of both val-ala and ala-val were also recorded over the same frequency region and at the same resolution for comparison.

Calculations

Previous studies have shown that zwitterionic amino acids do not exist as isolated monomers. A similar conclusion is expected to apply to the dipeptides. We have argued that the dielectric field of KBr is sufficient to stabilize the zwitterions.[19,20] This requires that to conduct meaningful calculations on the zwitterionic forms of amino acids and dipeptides, existing as monomeric entities, solvation effects must be included. Self-consistent reaction field (SCRF) theory can be used to study solvated molecules, in which the molecule is viewed as a solute in a continuum (solvent) with a uniform dielectric constant (reaction field). In the Onsager model, the solute occupies a spherical cavity. Other SCRF methods are available but have more limited applications.[21,22] With respect to vibrational frequency calculations, the Onsager approach has been shown to be as good, if not better, than any of the other methods.[22]

In recent continuing theoretical studies on glycine, the presence of specific alkali halide molecules has been shown to be sufficient to stabilize the zwitterions.[23] Similar observations have been made for the presence of specific water molecules.[24]

Ab initio molecular orbital calculations of the SCRF type using the Onsager dipole−sphere model were undertaken for zwitterionic val-ala and ala-val. Details of the calculations, which are implemented in the GAUSSIAN 98 packages,[25] have been previously reported.[13] In this work, geometry optimizations and vibrational frequency and absorption intensity predictions were undertaken at HF (Hartree−Fock) and DFT (density functional theory) levels. The DFT technique employed the Becke 3 (B3)[26] exchange functional, which was supplemented with the Lee, Yang, Parr (LYP)[27] correlation functional.

The majority of the calculations was performed with the 6-31G(d) basis set. This basis set is of double-ζ type with d functions added to the nonhydrogen atoms. In addition, some specific calculations were repeated at the HF level using the larger basis, 6-311++G(d,p). This basis is formed from the standard 6-31G(d) with the addition of extra polarization, correlation, and diffuse functions. In detail, it includes p type Gaussian polarization functions on each hydrogen atom; extra valence functions (triple-ζ) and core functions (single-ζ) for correlation; and four diffuse functions (s, p_x, p_y, p_z) on each nonhydrogen atom and one highly diffuse s function on each hydrogen atom. Such a basis is more successful in accounting for long-range interactions such as H-bonding.[22] However, it is recognized that the inclusion of the diffuse function on H atoms in general does not make a significant difference in accuracy.[22]

Input data for SCRF calculations include the cavity radius, a_0, and the dielectric constant, ϵ. The cavity radius cannot be directly determined from an ab initio calculation of the isolated (gas phase) zwitterion since the isolated zwitterion is not stable. In this study, the cavity radius was used as an adjustable parameter in order to reach the best agreement between predicted and observed spectra. Initial estimates were obtained from the isolated unionized molecules by standard SCF energy optimization runs. Values in the range of 4.8−5.2 Å were obtained for a number of conformers of the unionized ala-val. This suggested that a similar range of cavity radii be used for the SCRF/HF/6-31G(d) calculations on both val-ala and ala-val zwitterions. It was assumed that the cavity radius found to give the best spectral agreement for all of the conformers using the 6-31G(d) basis could also be used for the SCRF calculations with the larger 6-311++G(d,p) basis. The validity of this assumption was confirmed by a series of calculations using the larger basis and carried out for cavity radii in the range of 4.8−5.2 Å for the Tg2 conformer of val-ala. The dielectric constant for the KBr continuum was taken as 4.88.[28]

No geometrical constraints were imposed on the SCRF determinations of the optimized structures at either HF or DFT (B3LYP) levels. Starting from all possible geometries, a number of stationary points were obtained. To verify that these stationary points were indeed local minima, harmonic vibrational frequencies were calculated following the structure optimizations, by analytic second differentiation of the energy with respect to nuclear displacements. The DFT calculated spectra at the B3LYP/6-31G(d) level did not provide better agreement than the HF spectra nor did they add further insight; hence, they have not been reported in this work.

To allow comparison with the observed spectra, the raw predicted vibrational frequencies were all scaled using a single factor, namely, 0.9051 for the HF/6-311++G(d,p) and 0.9614 for B3LYP/6-31G(d). The frequency scaling corrects for the well-known systematic frequency overestimation due to lack of or incomplete inclusion of electron correlation.[29]

The simulations of the calculated spectra were achieved by assigning Lorentzian line shapes of 4 cm^{-1} width at half-height to all calculated bands using the AniMol 3.2 software and exported into SigmaPlot 2001 for Windows plotting program. The line widths were arbitrarily chosen to equal the instrumental resolution, although it is recognized that site effects mainly arising from zwitterion clusters, other than the predominant monomers, can also be expected to contribute. The band heights correspond to the calculated intensities.

Results and Discussion

Structures. Six different stationary points were found at the HF/6-31G(d) and B3LYP/6-31G(d) levels for both val-ala and ala-val, using cavity radii in the range of 4.6−5.2 Å. The six

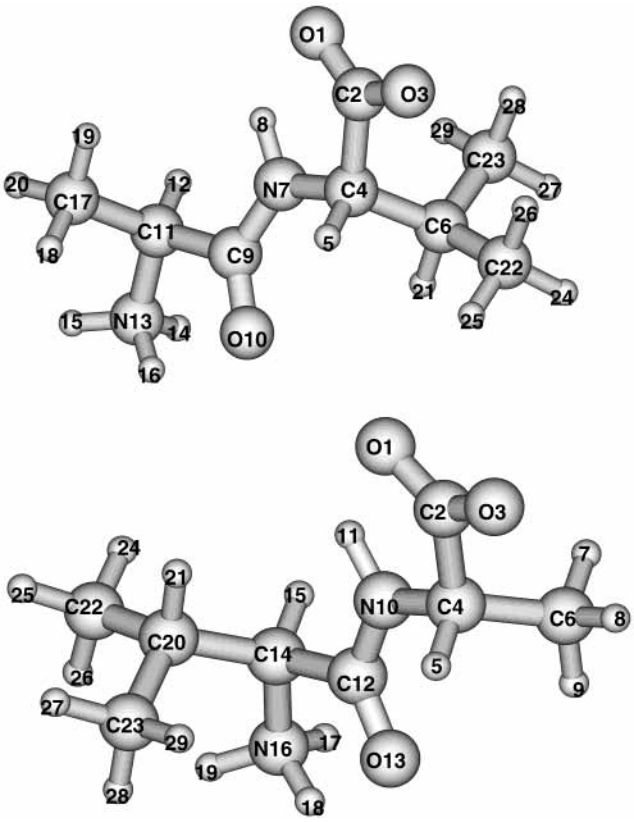

Figure 1. Optimized geometries (SCRF/HF/6-311++G(d,p), a_o = 5.0Å) of the Tg1 and Tg2 conformers of ala-val and val-ala, respectively.

local minima arise from the two possible cis/trans configurations about the CN bond of the amide linkage, labeled C and T, and the three possible rotations about the C−C bond of the valyl side chain. The latter three are labeled trans (t), gauche 1 (g1), and gauche 2 (g2), in accordance with the crystal structure work on L-valine by Torii and Iitaka.[30] The SCRF/HF/6-311++G-(d,p) optimized geometries of the Tg1 conformer of ala-val and the Tg2 conformer of val-ala zwitterions at a cavity radius of 5.0 Å are depicted in Figure 1 with the atom numbering used in the calculations.

The sensitivity of the conformer stabilities and vibrational spectra to cavity radius was investigated. Vibrational frequencies were calculated to verify that the six stationary points are indeed local minima. No imaginary frequencies were found for any of the above cavity radii, and accordingly, the theoretical existence of six stable conformers has been established. The SCRF calculations of both the HF and the DFT types gave the same order of energies for the six conformers at all cavity radii studied. With the larger 6-311++G(d,p) basis in the SCRF/HF calculations, all six conformers of val-ala were identified and their optimized geometries were determined, but for ala-val, only five conformers optimized to the zwitterionic form. The highest energy conformer for ala-val optimized to the neutral form for cavity radii of 5.0 Å and larger. For smaller cavity radii, it was not possible to get convergence for this conformer.

In our work, the final criterion in the choice of a specific cavity radius has been the achievement of optimum agreement between the predicted and the measured spectra for one or more conformers. A comparison of the vibrational frequencies of the measured DSD and calculated (SCRF/HF/6-31G(d)) spectra for all conformers showed that the best agreement is obtained for cavity radii near 5.0 Å. This was also shown to be true in structure/frequency calculations for the Tg2 conformer of val-ala using the larger basis. Hence, this cavity radius was used for all of the calculations with the larger basis and for the density functional approach.

The calculations, at all levels undertaken, have shown that the T conformers are more stable than the C conformers by several thousand cm^{-1} and that the Tg2 and Tg1 conformers are the most stable for val-ala and ala-val, respectively (Table 1). However, the small energy differences determined for the three T conformers make the latter predictions less secure.

These chiral molecules have two chiral centers each. For val-ala, C2C4N10C6 and C2C4H5C6 dihedral angles specify the absolute configuration of one chiral center while C12C14N16C20 and C12C14H15C20 dihedral angles specify the absolute configuration of the other. The former is positive and the latter is negative for each pair, for the L form of val-ala. By reversing the signs of all of the four dihedral angles, the D enantiomer is obtained, which will have the same IR properties as the L isomer. However, by reversing the sign of just one pair of dihedral angles, the diastereomers are obtained, and they have different spectral properties. Because the primary aim of this work was comparison of the calculated results with the experimental measurements, discussion of the calculations will be confined to the naturally occurring L enantiomer.

The key dihedral angles for all of the conformers of val-ala calculated at the SCRF/HF/6-311++G(d,p) level for a cavity radius of 5.0 Å are listed in Table 2, together with those determined by X-ray diffraction.[31]

The dihedral angles, H11N10C12O13 of val-ala and H8N7C9O10 of ala-val, are close to 180° for the trans and 0° for the cis forms. The peptide linkage formed by these four atoms is thus found to be approximately planar. To check the possibility of the existence of nonplanar structures, geometry optimizations were also carried out starting with angles for this dihedral of ±30, ±60, ±90, ±120, ±150, and 180°. In most of the cases, the geometry optimized to the more stable trans form. When the starting geometry had a dihedral angle in the range of 30 to −30°, the structure optimized to the cis form. Similar behavior was noted for the dihedrals ω(C14C12N10C4) and ω(C11C9N7C4) of val-ala and ala-val, respectively.

For the conformers arising from the three possible rotations about the C14C20 bond, the H15C14C20H21 dihedral angle is close to 180° for the trans, +60° for the gauche 1, and −60° for the gauche 2 forms of val-ala. In the same vein, the H5C4C6H21 dihedral angle is close to 180° for the trans, +60° for the gauche 1, and −60° for the gauche 2 forms of ala-val.

The comparison between the calculated values of the dihedral angles of the conformers of val-ala and the crystal structure data of Table 2 shows that a good match is obtained for the Tg2 conformer. In particular, a value of 176.0 for ω-(C14C12N10C4) indicates a trans structure in the crystal, while values of −71.5 and 53.6° for the dihedral angles N16C14C20C22 and N16C14C20C23, respectively, indicate the g2 conformation.

The majority of calculated bond lengths and angles is little changed among the conformers of the one isomer and could not be used to distinguish between them. The largest differences are seen to occur for the C2−C4 bond lengths where the T conformers are shorter than the C by about 0.01 Å. However, the H-bonded distances, O1···H11 for val-ala and O1···H8 for ala-val, showed much larger variations with different conformers, up to 0.06 Å. For val-ala, the C forms (1.98−1.99 Å) had shorter H-bonded distances than the T forms (2.04−2.05 Å), while for ala-val the results were mixed.

TABLE 1: Calculated Relative Energies (cm^{-1}) of the Different Conformers of Val-Ala and Ala-Val for a Range of Cavity Radii (Å)

	val-ala						ala-val					
level of theory (a_0)	Tg1	Tg2	Tt	Cg1	Cg2	Ct	Tg1	Tg2	Tt	Cg1	Cg2	Ct
HF/6-31G*(4.6)	355	0	477	4429	2731	3833	0	426	995	2960	4176	4687
HF/6-31G*(4.8)	296	0	461	4230	2576	3626	0	360	930	2749	3937	4273
HF/6-31G*(5.0)	249	0	448	4072	2460	3465	0	304	873	2581	3736	3928
HF/6-31G*(5.2)	212	0	437	3944	2372	3339	0	255	822	2447	3464	3634
B3LYP/6-31G*(5.0)	195	0	323	3452	1891	2980	0	321	579	2125	3139	3304
HF/6-311++G**(5.0)	429	0	502	4448	2744	3697	0	220	894	2809	3801	

TABLE 2: Key Dihedral Angles of the Conformers of Val-Ala Calculated for Cavity Radius of 5.0 Å at the SCRF/HF/6-311++G(d,p) Level

	Tg1	Tg2	Tt	Cg1	Cg2	Ct	crystal structure[31]
C2C4N10C6	122.7	122.6	122.8	121.2	121.8	121.8	
C2C4H5C6	−121.1	−121.0	−121.0	−118.0	−118.3	−118.3	
C12C14N16C20	124.3	123.9	121.8	122.5	121.8	119.4	
C12C14H15C20	−129.0	−126.2	−128.4	−130.6	−127.0	−129.6	
H11N10C12O13	−175.5	−175.2	−174.2	1.4	1.8	0.7	
H15C14C20H21	64.4	−64.1	173.1	58.2	−72.2	161.5	
ψ(N16C14C12N10)	159.9	167.3	148.1	142.5	155.2	138.5	162.9(6)
ω(C14C12N10C4)	176.2	177.2	175.2	−31.3	−23.5	−22.3	176.0(6)
ϕ(C12N10C4C2)	−162.1	−164.3	−160.9	−142.9	−153.4	−155.0	−150.6(6)
N16C14C20C22	65.8	−66.3	173.2	59.8	−73.6	161.1	−71.5(8)
N16C14C20C23	−167.5	60.8	−63.6	−173.0	53.1	−73.1	53.6(8)
N10C4C2O1	−5.8	−6.1	−6.0	−9.2	−6.4	−6.4	−28.2(9)

Similar observations were made for the relative bond lengths of the two isomers. The largest calculated bond length difference for the conformers of val-ala as compared to the conformers of ala-val is about 0.02 Å for the C4−C6 bond and a similar difference for the corresponding C14−C20 (val-ala) and C11−C17 (ala-val) bonds (Table 3).

A comparison of calculated bond lengths and angles of the Tg2 conformer of val-ala with the crystallographically determined data[31] is presented in Table 3. Similarly calculated results for the Tg1 conformer of ala-val are also included in the table, but no experimental data are available for it. It is seen that apart from the two CC bonds mentioned above, corresponding bonds and angles for the two conformers have very similar values and that agreement with the crystal structure data is good.

Spectra. The majority of calculated vibrational frequencies and intensities was found to be closely similar for all the conformers (Table 4). However, the calculations revealed that although differences are very small among conformers within each of the T and C categories, some larger differences exist between the two categories. This applies particularly to the NH deformation mode of both val-ala and ala-val (Table 4). In the DSD spectra of both isomers, a strong band is seen at ∼1525 cm^{-1}. In the calculated spectra for the T conformers, a strong band is predicted at this frequency, whereas for the C conformers the nearest band is calculated to be some 60 cm^{-1} distant.

The spectral observation that the conformer(s) present in the DSD sample is trans is in agreement with the computed relative stabilities, Table 1, and with the conformer identified in the crystal of val-ala. Further assignment of the DSD spectrum to one, or more, of the three T conformers is excluded by the small differences in their predicted spectra and the margins of uncertainty in their calculated values.

The observed IR absorption spectra of val-ala and ala-val zwitterions in KBr matrixes, obtained by the DSD technique, are shown in Figures 2 and 3, respectively. The normal KBr pellet spectra were measured and are also included in the figures. The simulated spectra (SCRF/HF/6-311++G(d,p), $a_o = 5.0$ Å) for the Tg1 and Tg2 conformers are included in the figures to illustrate the relatively good agreement with the DSD spectra and to underline the marked similarity of the calculated spectra of each conformer. Apart from only a few bands, Table 4, this spectral similarity extends to the C conformers.

TABLE 3: Comparison of Crystal Structure Data of Val-Ala with Calculated (SCRF/HF/6-311++G(d,p), $a_o = 5.0$Å) Bond Lengths and Angles of the Tg2 and Tg1 Conformers of Val-Ala and Ala-Val, Respectively

	val-ala		ala-val	
	Tg2	crystal structure[31]		Tg1
O1−C2	1.232	1.277(8)	O1−C2	1.232
O3−C2	1.228	1.241(8)	O3−C2	1.223
C2−C4	1.558	1.539(10)	C2−C4	1.562
C4−C6	1.528	1.518(10)	C4−C6	1.547
C4−N10	1.467	1.459(8)	C4−N7	1.468
N10−H11	1.001	0.88	N7−H8	1.002
N10−C12	1.315	1.322(8)	N7−C9	1.314
C12−O13	1.211	1.231(8)	C9−O10	1.210
C12−C14	1.544	1.528(10)	C9−C11	1.542
C14−H15	1.081	1.00	C11−H12	1.081
C14−N16	1.509	1.481(8)	C11−N13	1.507
N16−H17	1.007	0.91	N13−H14	1.008
N16−H18	1.019	0.91	N13−H15	1.008
N16−H19	1.007	0.91	N13−H16	1.018
C14−C20	1.543	1.522(9)	C11−C17	1.526
C20−H21	1.086		C6−H21	1.087
C20−C22	1.533	1.549(11)	C6−C22	1.531
C20−C23	1.533	1.536(10)	C6−C23	1.532
O1···H11	2.039	2.17	O1···H8	2.011
O13···H11	3.145		O10···H8	3.145
O13···H17	2.998		O10···H14	2.935
O13···H18	1.917	1.92	O10···H16	1.988
O1−C2−O3	129.6	125.5(7)	O1−C2−O3	129.6
O1−C2−C4	115.9	118.5(6)	O1−C2−C4	115.8
O3−C2−C4	114.5	116.0(7)	O3−C2−C4	114.6
C2−C4−C6	111.1	109.1(6)	C2−C4−C6	110.8
C2−C4−N10	108.4	110.8(5)	C2−C4−N7	108.0
C6−C4−N10	111.6	111.9(6)	C6−C4−N7	113.3
C4−N10−C12	124.9	119.6(6)	C4−N7−C9	125.3
N10−C12−O13	126.1	124.0(6)	N7−C9−O10	127.3
N10−C12−C14	116.5	116.4(6)	N7−C9−C11	115.8
O13−C12−C14	117.4	119.5(6)	O10−C9−C11	116.9
C12−C14−N16	104.6	106.0(5)	C9−C11−N13	105.0
C12−C14−C20	114.3	112.6(6)	C9−C11−C17	112.1
N16−C14−C20	111.4	112.1(6)	N13−C11−C17	109.7
C14−C20−C22	111.5	112.3(6)	C4−C6−C22	112.6
C14−C20−C23	112.9	112.2(6)	C4−C6−C23	113.0
C22−C20−C23	111.9	110.4(6)	C22−C6−C23	110.8

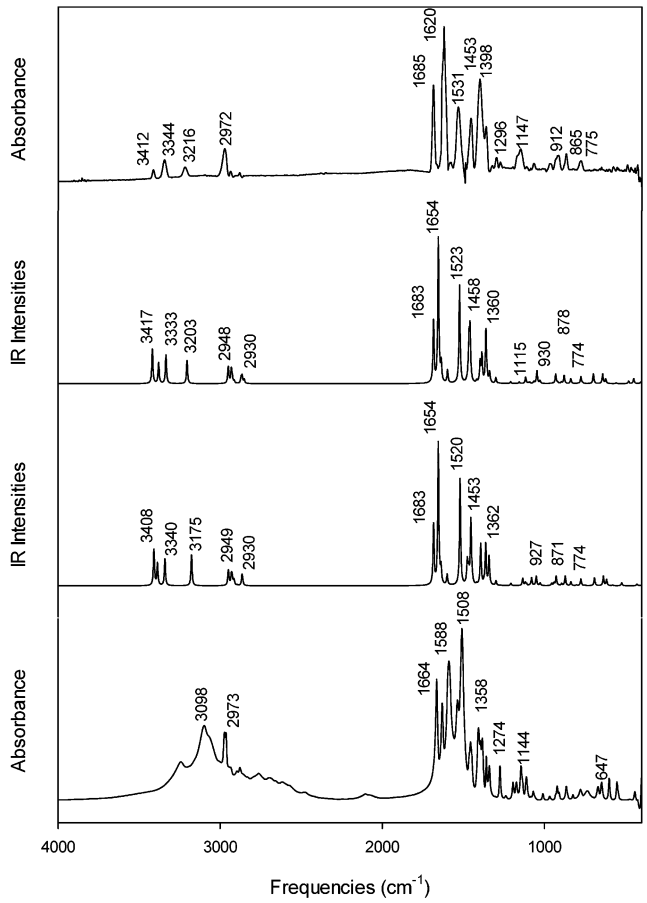

Figure 2. IR absorption spectra of zwitterionic val-ala obtained by (a) the DSD method; (b,c) the SCRF/HF/6-311++G(d,p) calculations for the Tg1 and Tg2 conformers, respectively; and (d) the KBr pellet method.

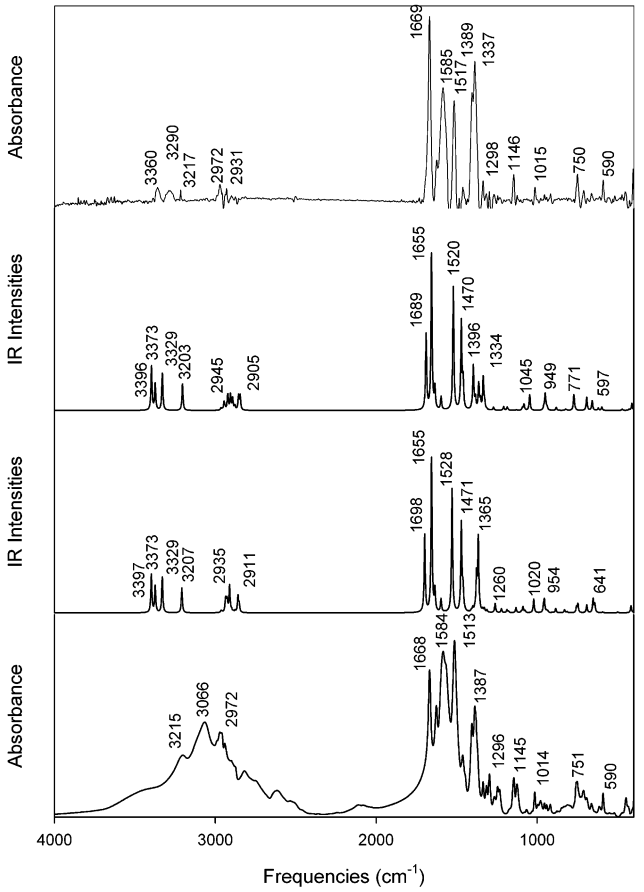

Figure 3. IR absorption spectra of zwitterionic ala-val obtained by (a) the DSD method; (b,c) the SCRF/HF/6-311++G(d,p) calculations for the Tg1 and Tg2 conformers, respectively; and (d) the KBr pellet method.

While the standard KBr pellet spectra of val-ala and ala-val are very similar, at least superficially, the much better resolved DSD spectra show small but significant differences. One of note concerns the band assigned to $\nu_a(CO_2^-)$. This suggests that the dispositions of the methyl and isopropyl groups, the side chains, do have subtle effects on the bonding of the dipeptides and on the nonbonded interactions. A comparison of the predicted (SCRF/HF/6-311++G(d,p)) frequencies, intensities, and assignments for the prominent bands of all conformers of both val-ala and ala-val with the DSD and KBr pellet measurements is given in Table 4.

Band assignments in the calculated spectra have been established from consideration of the normal coordinates. In the observed DSD spectra, the assignments have been determined from comparison with the predicted spectra and from consideration of the spectra of related molecules. It should be noted that most normal coordinates in the calculations are severely mixed in terms of the internal coordinates, and only the largest internal coordinate contribution is recorded in the tables. The mixing is most severe for the lower frequency bands, mainly those less than about 1200 cm^{-1}.

The frequencies, intensities, and assignments of some of the prominent bands in the DSD spectra, together with comparable measurements for the related molecules gly-ala, val-gly, and alanine, are presented in Table 5. The listed bands are characteristic of amino acid IR spectra and largely concern vibrations of the NH_3^+, CO_2^-, NH, and CO groups. Justification for the proposed assignments is given in the following. In the context of the table, some of the assignments for the related molecules have been reviewed and modified from those previously reported.

For each of the four dipeptides considered in Table 5, there are in theory four NH/NH_3^+ stretching type modes, as compared to three (NH_3^+) for the amino acid, alanine. For none of the dipeptides listed in the table have four resolved bands been observed. The calculations indicate that they should all be of similar intensities. This raises the questions of whether in the spectra of val-ala and ala-val one of the observed bands is in fact the overlap of two bands and furthermore whether one of the bands can be assigned to the NH stretch of the amide linkage. For val-ala, the highest frequency band (3412 cm^{-1}) of the three observed has been tentatively assigned to the NH stretch. A secure argument against assignment of this band to the NH_3^+ group cannot be made. However, it should be noted that none of the calculations, Table 4, has given an NH_3^+ stretch at frequencies greater than 3400 cm^{-1}, while they have done so for the NH stretch. Then, consideration of the calculated and observed intensities suggests that in the spectrum the second band, observed at 3344 cm^{-1}, is a composite of two bands. If correct, this would mean that all four bands have been located, supporting the assignment of the 3412 cm^{-1} to the NH stretch.

A similar pattern of three bands is seen for val-gly[20] but shifted some 70 cm^{-1} to lower frequencies relative to val-ala. This is in accord with the calculations that do predict lower frequencies for the NH/NH_3^+ stretches of val-gly. The standard KBr pellet spectra are of some help in this regard. For val-ala and ala-val, two broad features are seen at lower frequencies. That one of the two may be assigned to the amide linkage is

TABLE 4: Comparison of Calculated (SCRF/HF/6-311++G(d,p), a_o = 5.0Å) Vibrational Frequencies (Scaled, cm^{-1}) and Relative Intensities (Parentheses) for Prominent Bands of All Conformers of Val-Ala and Ala-Val Zwitterions with DSD and KBr Pellet Spectra[a]

				val-ala				
mode	Tg1	Tg2	Tt	Cg1	Cg2	Ct	DSD	KBr pellet
δCO_2^-	774(<1)	774(<1)	775(<1)	774(<1)	766(<1)	769(<1)	775(1)	778
δCH_3	1360(4)/	1362(3)/	1355(4)/	1390(1)	1388(1)	1390(1)	1360(3)	1358
$\nu_s CO_2^-$	/1396(1)	/1392(3)	/1392(2)	1355(1)	1351(3)	1351(3)	1398(7)	1407
$\Sigma\,\delta CH_3$	1458	1475	1485	1479	1475	1480	1454(4)	1456
δNH	1523(7)	1520(7)	1519(8)	1432(0)	1421(0)	1421(0)	1532(5)	1509
δNH_3^+	1465((2)	1453(5)	1456(3)	1465(2)	1469(1)	1460(1)	1454(4)	1456
δNH_3^+	1597(1)	1599(1)	1599(1)	1604(1)	1599(1)	1606(1)	1578(1)	1536
δNH_3^+	1636(1)	1637(1)	1632(1)	1632(1)	1634(1)	1632(1)	1660(sh)	1631
$\nu_a CO_2^-$	1654(10)	1654(10)	1654(10)	1663(10)	1661(10)	1662(10)	1620(10)	1589
νCO	1683(4)	1683(4)	1686(4)	1687(1)	1686(1)	1687(1)	1685(6)	1665
$\Sigma\,\nu CH_3$	2948	2949	2949	2951	2961	2955	2972(2)	2973
$\nu_s NH_3^+$	3203(2)	3175(2)	3227(1)	3236(1)	3221(1)	3232(1)	3216(1)	3073
$\nu_a NH_3^+$	3333(2)	3340(2)	3342(2)	3338(2)	3343(1)	3342(1)	3344(1)	3099
$\nu_a NH_3^+$	3378(1)	3386(2)	3385(2)	3382(1)	3387(1)	3384(1)	3344(1)	
νNH	3417(2)	3408(3)	3411(2)	3344(2)	3357(2)	3355(2)	3412(1)	3241

				ala-val				
mode	Tg1	Tg2	Tt	Cg1	Cg2	Ct	DSD	KBr pellet
δCO_2^-	771(1)	746(1)	757(1)	764(1)	736(<1)		750(2)	751
δCH	1362(2)	1365(5)/	1366(1)	1340(<1)	1345(<1)		1337(1)	1336
$\nu_s CO_2^-$	1396(3)	/1376(2)	1359(5)	1376(2)	1361(3)		1389(8)	1405
$\Sigma\,\delta CH_3$	1460	1461	1461	1457	1454		1463(1)	1463
δNH_3^+	1470(6)	1471(3)	1470(5)	1465(1)	1462(1)		1463(1)	1463
δNH	1520(8)	1528(8)	1529(8)	1448(1)	1473(1)		1517(6)	1514
δNH_3^+	1596(1)	1596(1)	1596(1)	1600(1)	1597(1)		1585(7)	1570
δNH_3^+	1635(1)	1634(1)	1634(1)	1633(1)	1634(1)		1625(2)	1626
$\nu_a CO_2^-$	1655(10)	1655(1)	1656(10)	1662(10)	1665(10)		1669(10)	1584
νCO	1689(2)	1698(5)	1694(5)	1687(1)	1685(2)		1684(sh)	1668
$\Sigma\,\nu CH_3$	2964	2963	2963	2988	3010		2972(1)	2972
$\nu_s NH_3^+$	3203(2)	3207(2)	3205(2)	3212(1)	3210(1)		3290(1)	
$\nu_a NH_3^+$	3329(2)	3329(2)	3329(2)	3332(1)	3335(1)		3290(1)	3066
$\nu_a NH_3^+$	3373(2)	3373(2)	3373(2)	3378(1)	3382(1)		3360(1)	
νNH	3396(3)	3397(3)	3400(3)	3356(2)	3389(1)		3388(<1)	3215

[a] Assignments are described in terms of ν, stretching; δ, deformation; s, symmetric; a, asymmetric; and sh, shoulder. Σ indicates a number of bands, and / indicates mixed assignment with /.

TABLE 5: Comparison of Some Vibrational Frequencies (cm^{-1}) and Intensities of Val-Ala and Ala-Val Obtained by the DSD and KBr Pellet Methods with Those of Gly-Ala, Val-Gly, and Alanine

	val-ala		ala-val		gly-ala		val-gly		alanine	
mode	DSD	KBr pellet	DSD	KBr pellet	DSD	KBr pellet	DSD	KBr pellet	DSD	KBr pellet
$\nu_s CO_2^-$	1398(7)	1407	1389(8)	1405	1396(3)	1408	1391(6)	1397	1397(4)	1410
δCH_3	1454(4)	1456	1463(1)	1463	1453(3)	1458	1468(1)	1472	1458(2)	1452
δNH	1532(5)	1509	1517(6)	1514		1536	1516(<1)	1498		
δNH_3^+	1578(1)	1536	1585(7)	1570			1574(6)	1585	1574(1)	
$\nu_a CO_2^-$	1620(10)	1589	1669(10)	1584	1598(10)	1563	1681(10)	1672	1617(10)	1594
δNH_3^+	1660(sh)	1631	1625(2)	1626			1621(1)	1621		1622
νCO	1685(6)	1665	1684(sh)	1668	1684(5)	1688	1671(sh)			
$\nu_s NH_3^+$	3216(1)	3073	3290(1)		3212(<1)		3103(1)		3143(1)	3086
$\nu_a NH_3^+$	3344(1)	3099	3290(1)	3066	3269(1)	3052	3270(2)		3249(2)	
$\nu_a NH_3^+$	3344(1)		3360(1)		3338(<1)		3270(2)		3314(1)	
νNH	3412(1)	3241	3388(<1)	3215		3218	3344(1)	3368		

supported by the observation of only one broad feature in the KBr pellet spectra of alanine[16] and glycine.[14] In the KBr pellet spectrum of val-gly,[20] a strong and well-resolved band is seen at 3368 cm^{-1}. It is at a comparable frequency to the highest DSD band providing further support for the assignments of the highest frequency bands in the spectra of val-ala and val-gly to the NH of the amide linkage.

For gly-ala,[19] the three bands (3338, 3269, and 3212 cm^{-1}), seen in the DSD spectrum, can be assigned to the NH_3^+ group, since they are quantitatively shifted upon deuteration. In the gly-ala study, only 60% total deuteration was achieved. The lack of more complete deuteration was attributed to the greater difficulty of exchanging the NH of the amide linkage. Hence, the NH stretch of the amide linkage should remain evident in the spectrum following such a degree of deuteration.

For ala-val, three resolved bands (3388, 3360, and 3290 cm^{-1}) are seen in the NH/NH_3^+ stretch region. The first is relatively very weak and has been assigned to the NH stretch, while the latter two have been assigned to the NH_3^+ group. The lower of the latter two is broad, indicative of overlap. The observed weakness and reduced frequency of the NH stretch of the amide linkage of ala-val relative to val-ala is in good agreement with the calculations. For alanine,[16] the three NH_3^+ stretches are seen but at lower frequencies.

In the region around 1600 cm^{-1}, val-ala displays two strong bands (1685 and 1620 cm^{-1}) in the DSD spectrum. Assignment

to the CO stretch (ν(CO)) and asymmetric stretch of the CO_2^- ($\nu_a(CO_2^-)$) groups, respectively, is consistent with the calculations and spectra of related molecules, although the calculated values of the latter for all conformers are higher, Table 4. For gly-ala, the bands are at 1684 and 1598 cm^{-1} in excellent agreement with the calculations, while for alanine one strong band is seen at 1617 cm^{-1}, close to the calculated value.

In the DSD spectrum of ala-val, strong bands are seen at 1669 and 1585 cm^{-1}, with a shoulder evident to the high frequency side of the former. According to the calculations for all conformers, the CO stretch is predicted to be at higher frequencies and smaller intensities than the asymmetric stretch of the CO_2^- group. Furthermore, the calculations predict that the two bands should be separated by about 20−40 cm^{-1} for all of the conformers. These predictions suggest that the strong band at 1669 cm^{-1} should be assigned to $\nu_a(CO_2^-)$ and the shoulder at about 1684 cm^{-1} to ν(CO). In this interpretation, the strong band at 1585 cm^{-1} must then be assigned to a deformation mode of the NH_3^+ group. This set of proposed assignments indicates that although the frequency of ν(CO) is unchanged, the frequency of $\nu_a(CO_2^-)$ is substantially increased in ala-val relative to val-ala, bringing it close to the calculated values of all conformers. In the KBr pellet spectra of the two isomers, the frequencies are only marginally different. We have no explanation for the difference in $\nu_a(CO_2^-)$ in the DSD spectra of the two isomers other than to note that the more bulky isopropyl group may better screen the carboxyl group from specific KBr interactions. Such specific interactions are not included in the Onsager dipole−sphere method and may explain why the observed frequency for $\nu_a(CO_2^-)$ of val-ala is less than the calculated value. It should also be mentioned that $\nu_a(CO_2^-)$ in general experiences larger frequency decreases than ν(CO) in going from the DSD sample to the crystal.[19] Crystal structure data indicate that the CO of the amide linkage is more sheltered from intermolecular interactions than the terminal CO_2^- group. For gly-ala in the crystal,[32] it is seen that the NH groups of the peptide linkages are involved in intermolecular H-bonding with the carboxyl oxygens. No such interactions are noted for the carbonyl oxygen of the peptide linkage.

The NH deformation is assigned to strong bands at 1532 and 1517 cm^{-1} for val-ala and ala-val, respectively, in good agreement with the calculated strong bands at 1523 and 1520 cm^{-1}. Comparison with gly-ala is not helpful in this respect since the NH deformation has not been identified. For val-gly, the strong band at 1574 cm^{-1} (calculated 1518) has been so assigned.

For the location of the NH_3^+ deformation bands, no consistent picture has emerged for the four dipeptides of Table 5. Assignments are proposed in Table 4 for val-ala and ala-val, but some of these must be regarded as tentative.

The CO_2^- symmetric stretch, $\nu_s(CO_2^-)$, is assigned to the strong bands at 1398 and 1389 cm^{-1} for val-ala and ala-val, respectively. These frequencies are very close to the values for the other molecules in Table 5. They change only little upon N-deuteration. The calculated frequencies are a little low as compared to the measurements, a fact also noted for gly-ala. The calculated intensities are largely in agreement with the observed strong bands.

A band of moderate intensity, common to the spectra of amino acids and dipeptides containing the methyl group, is assigned to a deformation mode of the CH_3 group. It is almost unchanged by N-deuteration and is observed at about 1460 cm^{-1}. For val-ala and ala-val, it may also contain one of the NH_3^+ deformations.

The amino acids and dipeptides are characterized by a band of medium intensity near 750 cm^{-1}, which can be attributed to deformation of the CO_2^- group. In our DSD spectra, bands are identified at 775 and 750 cm^{-1} for val-ala and ala-val, respectively.

Finally, a band of medium intensity is observed in all of the spectra, DSD and KBr pellet, at about 1145 cm^{-1}. There is no good match with the calculations, but assignment to νCN is in best agreement with the calculations.

Conclusion

Val-ala and ala-val zwitterions are isomers and are expected to display similar vibrational absorption spectra. This is indeed evident in the almost identical spectra measured by the KBr pellet method where only small differences are noted in some of the bands, particularly those below about 1300 cm^{-1}. However, with the better resolution achieved in the DSD spectra, small but significant differences are also observed for some of the prominent bands, in particular $\nu_a(CO_2^-)$, suggesting that the dispositions of the side chains do have subtle effects on the bonding.

Six and five conformers, respectively, were calculated to exist for val-ala and ala-val at the highest levels of theory used. The best agreement between the calculated and the observed spectra was noted for the trans conformers consistent with the computed relative stabilities. This suggests that the val-ala species produced by the DSD technique is possibly the Tg2 conformer in agreement with the species identified in the crystal.

The clear similarities in the spectra of val-ala, ala-val, gly-ala, val-gly, and alanine confirm that most of the prominent bands in the spectra can be attributed to vibrations localized largely on the carboxyl and amino groups. For these molecules with predominantly nonpolar side chains, bands that can be assigned to the side chains are in general weaker. However, steric effects cannot be excluded, and the more bulky isopropyl group may partially screen the carboxyl group of ala-val from specific KBr interactions. This explanation has been proposed for the poorer agreement between theoretical and DSD values for the $\nu_a(CO_2^-)$ frequency of val-ala. For ala-val, the corresponding agreement is excellent.

The calculated structures reveal that the side chains are not characterized by any short nonbonded distances, and accordingly, for the side chains, significant nonbonded intramolecular interactions, and therefore reduced vibrational frequencies, can be excluded.

Acknowledgment. The Australian Research Council is thanked for its support of this work. The ab initio calculations were carried out on the Silicon Graphics Power Challenge of the ANU Supercomputer Facility and the Compaq Alpha Server SC of the APAC National Facility. R.J. thanks the Department of Chemistry for its hospitality and the Australian National University for a Visiting Fellowship.

References and Notes

(1) Iijima, K.; Tanaka, K.; Onuma, S. *J. Mol. Struct.* **1991**, *246*, 257.
(2) Iijima, K.; Nakano, M. *J. Mol. Struct.* **1991**, *465*, 255.
(3) Reva, I. D.; Stepanian, S. G.; Plokhotnichenko, A. M.; Radchenko, E. D.; Sheina, G. G.; Blagoi, Y. P. *J. Mol. Struct.* **1994**, *318*, 1.
(4) Reva, I. D.; Plokhotnichenko, A. M.; Stepanian, S. G.; Ivanov, A. Y.; Radchenko, E. D.; Sheina, G. G.; Blagoi, Y. P. *Chem. Phys. Lett.* **1995**, *232*, 141.
(5) Suenram, R. D.; Lovas, F. J. *J. Mol. Spectrosc.* **1978**, *72*, 372.
(6) Suenram, R. D.; Lovas, F. J. *J. Am. Chem. Soc.* **1980**, *102*, 7180.
(7) Godfrey, P. D.; Firth, S.; Hatherley, L. D.; Brown, R. D.; Pierlot, A. P. *J. Am. Chem. Soc.* **1993**, *115*, 9687.

(8) Godfrey, P. D.; Brown, R. D. *J. Am. Chem. Soc.* **1995**, *117*, 2019.
(9) Grenie, Y.; Garrigou-Lagrange, C. *J. Mol. Spectrosc.* **1972**, *41*, 240.
(10) Rosado, M. T. S.; Duarte, M. L. R. S.; Fausto, R. *J. Mol. Struct.* **1997**, *410*−*411*, 343.
(11) Ding, Y.; Krogh-Jespersen, K. *Chem. Phys. Lett.* **1992**, *199*, 261.
(12) Yu, D.; Armstrong, D. A.; Rauk, A. *Can. J. Chem.* **1992**, *70*, 1762.
(13) Cao, X.; Fischer, G. *Spectrochim. Acta A* **1999**, *55A*, 2329.
(14) Cao, X.; Fischer, G. *Proceedings of the 22nd Annual Meeting of Australian Society for Biophysics*; Australian National University: Canberra, 1998.
(15) Cao, X.; Fischer, G. *J. Phys. Chem. A* **1999**, *103*, 9995.
(16) Cao, X.; Fischer, G. *Chem. Phys.* **2000**, *255*, 195.
(17) Cao, X.; Fischer, G. *J. Mol. Struct.* **2000**, *519*, 153.
(18) Cao, X.; Fischer, G. *J. Phys. Chem. A* **2002**, *106*, 41.
(19) Jacob, R.; Fischer, G. *J. Mol. Struct.* **2002**, *613*, 175.
(20) Fischer, G.; Jacob, R.; Cao, X. *Chem. Phys.* **2001**, *263*, 243.
(21) Bonaccorsi, R.; Palla, P.; Tomasi, J. *J. Am. Chem. Soc.* **1984**, *106*, 1945.
(22) Foresman, J. B.; Frisch, Æ. *Exploring Chemistry with Electronic Structure Methods*, 2nd ed.; Gaussian, Inc.: Pittsburgh, PA, 1996.
(23) Fischer, G. Unpublished work, 2002.
(24) Jenson, J. H.; Gordon, M. S. *J. Am. Chem. Soc.* **1995**, *117*, 8159.
(25) Frisch, M. J.; Trucks, G. W.; Schlegel, H. B.; Scuseria, G. E.; Robb, M. A.; Cheeseman, J. R.; Zakrzewski, V. G.; Montgomery, J. A., Jr.; Stratmann, R. E.; Burant, J. C.; Dapprich, S.; Millam, J. M.; Daniels, A. D.; Kudin, K. N.; Strain, M. C.; Farkas, O.; Tomasi, J.; Barone, V.; Cossi, M.; Cammi, R.; Mennucci, B.; Pomelli, C.; Adamo, C.; Clifford, S.; Ochterski, J.; Petersson, G. A.; Ayala, P. Y.; Cui, Q.; Morokuma, K.; Malick, D. K.; Rabuck, A. D.; Raghavachari, K.; Foresman, J. B.; Cioslowski, J.; Ortiz, J. V.; Stefanov, B. B.; Liu, G.; Liashenko, A.; Piskorz, P.; Komaromi, I.; Gomperts, R.; Martin, R. L.; Fox, D. J.; Keith, T.; Al-Laham, M. A.; Peng, C. Y.; Nanayakkara, A.; Gonzalez, C.; Challacombe, M.; Gill, P. M. W.; Johnson, B. G.; Chen, W.; Wong, M. W.; Andres, J. L.; Head-Gordon, M.; Replogle, E. S.; Pople, J. A. *Gaussian 98*; Gaussian, Inc.: Pittsburgh, PA, 1998.
(26) Becke, A. D. *J. Chem. Phys*. **1992**, *97*, 9173; **1993**, *98*, 5648.
(27) Lee, C.; Yang, W.; Parr, R. G. *Phys. Rev. B* **1988**, *37*, 785.
(28) *Handbook of Chemistry and Physics*, 80th ed.; Lide, D. R., Ed.; CRC Press LLC: Boca Raton, 1999.
(29) Scott, A. P.; Radom, L. *J. Phys. Chem.* **1996**, *100*, 16502.
(30) Torii, K.; Iitaka, Y. *Acta Crystallogr. B* **1970**, *26*, 1317.
(31) Gorbitz, C. H.; Gundersen, E. *Acta Crystallogr. C* **1996**, *C52*, 1764.
(32) Wang, A. H.; Paul, I. C. *Acta Crystallogr. C* **1979**, *C8*, 269.